WHISTLER MODE INSTABILITY IN A LORENTZIAN (κ) MAGNETOPLASMA IN THE PRESENCE OF PERPENDICULAR A.C. ELECTRIC FIELD AND COLD PLASMA INJECTION

A. K. TRIPATHI and K. D. MISRA
Department of Applied Physics, Institute of Technology, Banaras Hindu University, Varanasi-221 005, India

(Received 4 April 2001; Accepted 21 March 2002)

Abstract. The dielectric tensor, modified plasma dispersion function and dispersion relation for Whistler mode instability in an infinite magnetoplasma are obtained in the case of cold plasma injection to background hot anisotropic generalized bi-Lorentzian (κ) plasma in the presence of external perpendicular a.c. electric field. The method of characteristics solutions using perturbed and unperturbed particle trajectories have been used to determine the perturbed distribution function. Integrals and modified plasma dispersion function $Z_\kappa^*(\xi)$ are reduced in power series expansion form. Numerical methods using computer technique have been used to obtained temporal growth rate for magnetospheric plasma at geostationary height. The bi-Lorentzian (κ) plasma is reducible to various forms of distribution function by changing the spectral index κ. The results of bi-Lorentzian (κ) plasma are compared with those of bi-Maxwellian plasma. It has been found that the addition of cold plasma injection gives different frequency spectra. The a.c. frequency of moderate amplitude increases the growth rate and instability in $\bar{\mathbf{K}}$ space to lower range. Growth rate maximum is not affected by a.c. frequencies. However, it shifts the maximum to lower $\bar{\mathbf{K}}$ space in both cases, rather than on the variation of the magnitude. Thus a physical situation like this may explain emission of various high frequency whistler emissions by cold plasma injection. The potential application of controlled plasma experiments in the laboratory and for planetary atmosphere are indicated.

1. Introduction

In many physical situations of geophysical and astrophysical plasma the distribution function contains a finite drift relative to the centre of momentum frame. The field aligned current carried by thermal electron and ion beams associated with field aligned electric potential drop along auroral field lines are the best examples of beam plasma and electric field system. In such cases field aligned beam can provide an additional source of free energy for the instabilities and growth of plasma waves. However, many times presence of perpendicular fluctuating electric field gives differential mobilities to the electron and ion beam propagating parallel to the magnetic field. These changes often become a strong additional source of energy in addition to any other existing source of free energy plasma wave instabilities (Summers and Thorne, 1987). It has long been known that the whistler mode instability can be generated by an electron temperature anisotropy (Kennel and Petschek, 1966). Gary and Madland (1985) have performed a de-

Earth, Moon and Planets **88:** 131–153, 2002.

tailed parametric study of electron fire-hose and whistler instabilities excited by electron temperature anisotropies. Their results indicate that the maximum growth rates of these instabilities are very sensitive to the background plasma parameters. The electron beam instabilities, linear and non-linear stages, have been extensively studied theoretically (e.g., Briggs, 1964; Neubert and Banks, 1992) and via computer simulations (e.g., Cairns and Nishikawa, 1989; Dum, 1990a,b). Whistler waves have also been studied extensively (e.g., Helliwell, 1965; Cuperman and Stemlieb, 1974; Sazhin, 1993), in particular, electron beam driven whistler waves (Misra et al., 1978; Omura and Matsumoto, 1988a,b; Nishikawa et al., 1994). Sazhin and Sazhina (1988) and Misra and Pandey (1995) studied the analytical solution for the whistler mode instabilities in the presence of hot electron beam with loss-cone index using generalized background bi-Maxwellian plasma. Cuperman and Landau (1974) and Misra and Singh (1980) studied the effect of cold plasma injection on the whistler mode instability in an anisotropic warm bi-Maxwellian magnetoplasma. Recently, the particle and fields measurements were used to study in the inner magnetosphere from the DMSPF8 and CRRES satellites (Maynard et al., 2000). Substantial increase in the energetic electron precipitation could be achieved by injection of a modest amount of cold plasma into the radiation belt (Brice, 1970; Brice and Lucas, 1971). Hypothetical experiments were used to analyse the enhancement in ULF BMC and VLF BMC noise by lithium and barium injection (Cornwall, 1974; Liemohn, 1974). Later on Ganguli et al. (1984) studied the temporal evolution of whistler growth in a cold plasma injection experiment suited to Active Magnetospheric Particle Tracer Explorers (AMPTE) satellite parameters.

In a series of papers, Misra and Singh (1977, 1980) and Misra et al. (1979) discussed the role of a d.c. parallel electric field in the generation of whistler mode instability including injection of cold plasma to bi-Maxwellian plasma. Recently, the effect of an a.c. electric field on the whistler mode instability in the magnetosphere was studied (Misra and Haile, 1993). This study was further generalized for a distribution function having Maxwellian plasma and a distribution having a varying loss-cone index with a positive slope region in the direction perpendicular to the magnetic field and time-varying cold plasma injection in the presence of a parallel a.c. field to the magnetic field (Misra and Haile, 2001a,b). Whistler wave generations by thermal electrons are especially influenced, in case of generalized bi-Lorentzian (κ) plasma rather than for a bi-Maxwellian plasma (Mace, 1999). Most natural space plasmas possess the continuous presence of a non-Maxwellian high energy tail component, that can best be modeled by a generalized bi-Lorentzian (κ) distribution function also known as κ distribution function (e.g., Lui and Krimigis, 1981; Vasyliunas, 1968; Chirston et al., 1988). The origin of the high-energy tail is not well understood, it is probably caused by stochastic acceleration processes that involve plasma waves (e.g., Hasegawa et al., 1985). In this distribution function, characterization is done by spectral index κ, which for different spectral indexes assumes different distribution function such as inverse

power-law tail (distribution $\propto$ (particle energy)$^{-(\kappa+1)}$) and to bi-Maxwellian distribution function and Maxwellian distribution function in the limit of $\kappa \to \infty$. The generalized bi-Lorentzian (κ) distribution has been considered extensively by various workers for explaining the whistler wave in planetary magnetosphere, solar wind, astrophysical phenomena and Earth's magnetosphere (Summers and Thorne, 1991, 1992; Summers et al., 1994).

Therefore, the purpose of this paper is to examine the whistler mode instability in the presence of cold plasma injection to background hot generalized bi-Lorentzian (κ) plasma with spectral index κ in the presence of perpendicular a.c. field using the perturbed and unperturbed particle trajectories, by method of characteristics. In Section 2 the element of dielectric tensor and the resulting dispersion relation, for whistler mode waves having the effect of cold plasma injection on background hot generalized bi-Lorentzian (κ) plasma in the presence of perpendicular electric field is given. The details of dispersion relation and evaluation of growth rate for bi-Lorentzian (κ) plasma as well as bi-Maxwellian plasma (under the limit $\kappa \to \infty$) are done by numerical procedures of computer techniques instead of bringing the growth rate in analytical form considering only two terms using simple asymptotic expansion of unmodified plasma dispersion function. Various physical aspects of hot plasma, cold plasma injection and a.c. electric field for different spectral indexes κ have been included in numerical calculations. The plasma dispersion function also gets modified in the presence of perpendicular a.c. electric field, as well as given integrals in elements of dielectric tensors also get modified and are solved by using the expansion of power series in the limit of $\lambda \to 0$. Results and Discussions are given in Section 3. Section 4 deals with Conclusions.

2. Detail Derivation of Dielectric Tensor and Dispersion Relation with Injected Cold Electron Plasma

The plasma under consideration is of infinite extent, spatially homogeneous collisionless, anisotropic, subjected to an external magnetic field $\mathbf{B}_0 = (B_0\hat{e}_z)$ and an electric field $\mathbf{E}_{0x} = E_0 \sin \nu t \hat{e}_x$. The distribution function is kept in the form of f_0 and is retained throughout which later on will assume the form of generalized Lorentzian (κ) distribution. The propagation is in x-z plane. $\mathbf{k}_\perp$ is the wave vector along x-axis and $\mathbf{k}_\parallel$ is the wave vector along the external magnetic field. In order to obtain the general dielectric tensor and dispersion relation for oblique propagation, the Vlasov–Maxwell equations are linearized for spatially homogeneous plasma by small perturbations in electric and magnetic wave fields and the distribution function, where $\mathbf{E}_1$, $\mathbf{B}_1$ and f_{s_1} are perturbed quantities and are assumed to have harmonic dependence in f_{s_1}, $\mathbf{B}_1$ and $\mathbf{E}_1 \cong \exp i(\mathbf{k}.\mathbf{r}-\boldsymbol{\omega}\mathbf{t})$. The approximation $E_0 \cos(\mathbf{k_0}.\mathbf{r} - \nu t) \simeq \mathbf{E_0} \cos \nu t$ naturally puts a limitation on the size of the spatial region over which the field can be treated as uniform, $\mathbf{k}_0 L \leq 1$, where L is the char-

acteristic dimension and k_0 is the wave number of pump satisfying $c^2\mathbf{k}^2 = c^2\mathbf{k}_0^2$. The calculations are valid within the characteristic dimension (Prasad, 1968).

In the following the a.c. pump frequency ν is included via particle trajectory. The particle trajectories and the unperturbed velocities are evaluated neglecting integration constant in Equations (6)–(7) of Misra and Pandey (1995) and is written as

$$\begin{aligned}
\mathbf{v}_{0x} &= \mathbf{v}_x \cos\omega_{c_s}t' - \mathbf{v}_y \sin\omega_{c_s}t' + \left\{\frac{\nu\Gamma_x}{(\omega_{c_s}^2 - \nu^2)}\right\}\cos\nu t' \\
\mathbf{v}_{0y} &= \mathbf{v}_x \sin\omega_{c_s}t' - \mathbf{v}_y \cos\omega_{c_s}t' - \left\{\frac{\nu\Gamma_x}{(\omega_{c_s}^2 - \nu^2)}\right\}\sin\nu t' \qquad (1)\\
\mathbf{v}_{0z} &= \mathbf{v}_z
\end{aligned}$$

and

$$\begin{aligned}
\mathsf{X}_o &= X + \mathbf{v}_y/\omega_{c_s}\frac{1}{\omega_{c_s}}[\mathbf{v}_x \sin\omega_{c_s}t' - \mathbf{v}_y\cos\omega_{c_s}t'] \\
&\quad + \frac{\Gamma_x}{\omega_{c_s}}\left[\frac{(\omega_{c_s}\sin\nu t' - \nu\sin\omega_{c_s t'})}{(\omega_{c_s}^2 - \nu^2)}\right] \\
\mathsf{Y}_o &= Y + \mathbf{v}_x/\omega_{c_s} - \frac{1}{\omega_{c_s}}[\mathbf{v}_x\sin\omega_{c_s}t' - \mathbf{v}_y\cos\omega_{c_s}t'] \\
&\quad + \frac{\Gamma_x}{\nu\omega_{c_s}}\left[1 + \left\{\frac{(\nu^2\cos\omega_{c_s}t' - \omega_{c_s}^2\cos\nu t'}{(\omega_{c_s}^2 - \nu^2)}\right\}\right] \\
\mathsf{Z}_o &= Z - \mathbf{v}_z t', \qquad (2)
\end{aligned}$$

where Γ_x and ν are the magnitude and frequency of the a.c. signal respectively, with the gyrofrequency ω_{c_s} and plasma frequency ω_{p_s} given as

$$\omega_{c_s} = \frac{q_s\mathbf{B}_0}{m_s c}, \quad \omega_{p_s}^2 = \frac{4\pi N_{0s}q^2}{m_s},$$

where q_s, m_s and N_{0s} are respectively particle charge, mass and number density of species s. Note that the gyrofrequency ω_{c_s} (and hence the variable λ_1) contains the sign of the particle charge.

The zero-order and the first-order quantities are denoted by the subscripts 0 and 1. The zero-order Boltzman distribution function is given as

$$\frac{\partial f_{os}}{\partial t} + \frac{e_s}{m_s}[\mathbf{E}_0\sin\nu t + (\mathbf{v}_0\times\mathbf{B}_0)]\frac{\partial f_{os}}{\partial v} = 0, \qquad (3)$$

$$\frac{\partial f_{os}}{\partial t} + \frac{e_s}{m_s}[\mathbf{E}_0 \sin \nu t + \mathbf{v}_{0x}.\omega_{cs} - \mathbf{v}_{0y}.\omega_{cs}]\frac{\partial f_{os}}{\partial \mathbf{v}_\parallel} = 0. \tag{4}$$

If zero-order particle distribution function $f_{os}(\mathbf{v})$ for the background warm plasma is taken to be a bi-Lorentzian (κ) as given below,

$$f_{0s}^{\kappa}(v) = \frac{1}{\pi^{3/2}\theta_{\perp_s}^2\theta_{\parallel_s}\kappa^{3/2}}\frac{\Gamma(\kappa+1)}{\Gamma\left(\kappa-\frac{1}{2}\right)}\left[1 + \frac{\mathbf{v}_{0z}^2}{\kappa\theta_{\parallel_s}^2} + \frac{\mathbf{v}_{0x}^2 + \mathbf{v}_{0y}^2}{\kappa\theta_{\perp_s}^2}\right]^{-(\kappa+1)}, \tag{5}$$

with associated effective thermal speeds parallel and perpendicular to the ambient magnetic field as

$$\theta_{\parallel_s} = [(2\kappa - 3)\kappa]^{1/2}(T_{\parallel_s}/m_s)^{1/2}$$

$$\theta_{\perp_s} = [(2\kappa - 3)\kappa]^{1/2}(T_{\perp_s}/m_s)^{1/2}$$

and the temperature anisotropy $A_{T_s}^{\kappa}$ defined by

$$A_{T_s}^{\kappa} = \frac{T_{\perp_s}}{T_{\parallel_s}} - 1 = \frac{\theta_{\perp_s}^2}{\theta_{\parallel_s}^2} - 1.$$

κ is the spectral index (the parameter κ generally takes on positive integral values ≥ 2), Γ is the gamma function. Substituting the values of unperturbed velocities v_{0x}, v_{0y} and v_{0z} from Equation (1) in f_0 one can easily see that this zero-order distribution function satisfy the zero-order Boltzman Equation (4). Now the first-order Boltzman equation is given as

$$\frac{\partial f_{s_1}}{\partial t} + \mathbf{v}\frac{\partial f_{s_1}}{\partial \mathbf{r}} + \frac{F}{m_s}\frac{\partial f_{s_1}}{\partial \mathbf{v}} = S(\mathbf{r}, \mathbf{v}, t), \tag{6}$$

where force is defined as $\mathbf{F} = m\,\mathrm{d}\mathbf{v}/\mathrm{d}t$ and c is the velocity of light in vacuum.

$$\mathbf{F} = e_s[E_0 \sin \nu t + \mathbf{v} \times \mathbf{B}_0]. \tag{7}$$

The particle trajectories are obtained by solving the equation of motion defined in Equation (7) and obtained in detail in Equations (1)–(2) and S ($\mathbf{r}$, $\mathbf{v}$, t) is defined as

$$S(\mathbf{r}, \mathbf{v}, t) = \frac{-e_s}{m_s}[\mathbf{E}_1 + (\mathbf{v} \times \mathbf{B}_1)]\frac{\partial f_{os}}{\partial \mathbf{v}} = 0, \tag{8}$$

where s denotes species.

The method of characteristics solutions is used to determine the perturbed distribution function f_{s_1}, which is obtained from Equation (6) as

$$f_{s_1}(\mathbf{r}, \mathbf{v}, t) = \int_0^\infty S\{\mathbf{r}_0(r, \mathbf{v}, t'), \mathbf{v}_0(\mathbf{r}, \mathbf{v}, t'), t - t'\}\,\mathrm{d}t', \tag{9}$$

we have transformed the phase space coordinates system from $(\mathbf{r}, \mathbf{v}, t)$ to $(\mathbf{r}_0, \mathbf{v}_0, t - t')$ and $\tau = t - t'$. The wave propagation is in x-z plane defined as

$$\mathbf{k} = [\mathbf{k}_\perp \hat{e}_x, 0, \mathbf{k}_\parallel \hat{e}_z] \tag{10}$$

$$S(\mathbf{r}, \mathbf{v}, t) = \frac{-e_s}{\omega m_s} E^{I(\mathbf{k}.\mathbf{r}-\omega t)}[(\omega - \mathbf{k}.\mathbf{v})\mathbf{E}_1 + (\mathbf{v}.\mathbf{E}_1)\mathbf{k}]\frac{\partial f_{0s}}{\partial \mathbf{v}}. \tag{11}$$

By transformation of coordinates, Equation (8) can be written in terms of perturbed quantities as

$$\begin{aligned} S(\mathbf{r}_0, \mathbf{v}_0, t - t') \;=\; & \frac{-e_s}{m_s \omega} E^{i[k.r_0(r,\mathbf{v},t')-\omega(t-t')]} \\ & \times[(\omega - \mathbf{k}.\mathbf{v}_0)\mathbf{E}_1 + (\mathbf{v}_0.\mathbf{E}_1)\mathbf{k}]\frac{\partial f_{0s}}{\partial \mathbf{v}}. \end{aligned} \tag{12}$$

After substituting the Equations (1) and (2) into Equation (12) and doing some lengthy algebraic simplifications, one obtains (Misra and Haile, 1993; Misra and Pandey, 1995) as

$$\begin{aligned} S(\mathbf{r}_0, \mathbf{v}_0, t - t') \;=\; & \frac{-e_s}{m_s \omega} e^{i(\mathbf{k}.\mathbf{r}-\omega t)} \sum_{m,n,p,q=-\infty}^{\infty} \\ & \times J_m(\lambda_1) J_n(\lambda_1) J_p(\lambda_2) J_q(\lambda_3) \\ & \times \exp i(m - n)\alpha \exp i(\omega - \mathbf{k}_\parallel \mathbf{v}_\parallel - (n + q)\omega_{c_s} \\ & + p\nu)t' \left\{ \frac{1}{\mathbf{v}_\perp} \frac{\partial f_0}{\partial \mathbf{v}_\perp} \left[(\omega - \mathbf{k}_\parallel \mathbf{v}_\parallel)\mathbf{E}_\perp \mathbf{v}_\perp \cos(\omega_{c_s} t' + \theta) \right. \right. \\ & \left. + (\omega - \mathbf{k}_\parallel \mathbf{v}_\parallel)] + \frac{\mathbf{E}_\perp \Gamma_x}{\omega_{c_s}^2 - \nu^2}[-\nu \cos \right. \\ & \times(\omega_{c_s} t' + \alpha \pm \theta) + \nu \cos \nu t' \cos(\alpha + \theta) \\ & \left. -\omega_{c_s} \sin \nu t' \sin(\alpha \pm \theta)] \right\} + \frac{\partial f_0}{\partial \mathbf{v}_\parallel}[\omega - \mathbf{k}_\perp \mathbf{v}_\perp \cos \\ & \times(\omega_{c_s} t' + \alpha) + \mathbf{k}_\parallel \mathbf{v}_\perp \mathbf{E}_\perp \cos(\omega_{c_s} t' \pm \theta) \\ & - \frac{\mathbf{k}_\parallel \mathbf{E}_\perp \nu \Gamma_x}{\omega_{c_s}^2 - \nu^2} \cos(\omega_{c_s} t' + \alpha \pm \theta) - \frac{\mathbf{k}_\perp \mathbf{E}_\parallel \nu \Gamma_x}{\omega_{c_s}^2 - \nu^2} \\ & \times(\cos \nu t' - \cos \omega_{c_s} t') + \frac{\mathbf{k}_\parallel \mathbf{E}_\perp \nu \Gamma_x}{\omega_{c_s}^2 - \nu^2} \\ & \left. \times\{\nu \cos \nu t' \cos(\alpha \pm \theta) - \omega_{c_s} \sin \nu t' \sin(\alpha \pm \theta)\} \right], \end{aligned} \tag{13}$$

where the Bessel identity $e^{i\lambda \sin\phi} = \sum_{K=-\infty}^{\infty} J_K(\lambda) e^{iK\phi}$ has been used.

Now one can write perturbed distribution function f_{s_1} after time integration of Equation (13) giving rise to the perturbed distribution function as

$$\begin{aligned} f_{s_1}(x,\mathbf{v},t) \;=\; & -\frac{ie_s}{m_s\omega}\sum_{m,n,p,q=-\infty}^{+\infty} \\ & \times\frac{J_m(\lambda_1)J_n(\lambda_1)J_p(\lambda_2)J_q(\lambda_3)e^{-i(m-n)\alpha}}{\omega-\mathbf{k}_\parallel\mathbf{v}_\parallel-(n+q)\omega_{c_s}+p\nu} \\ & \times\left[\left\{\frac{n}{\lambda_1}C\mathbf{E}_{1x}-i\frac{J_n'}{J_n}C\mathbf{E}_{1y}+H\mathbf{E}_{1z}\right\}+\left\{\nu\left(\frac{p}{\lambda_2}-\frac{n}{\lambda_1}\right)\right.\right. \\ & \left.\left.\times D\mathbf{E}_{1x}-i\left(\omega_{c_s}\frac{J_p'}{J_p}D\right)\mathbf{E}_{1y}+G\left(\frac{p}{\lambda_2}-\frac{n}{\lambda_1}\right)\mathbf{E}_{1z}\right\}\right]. \end{aligned} \tag{14}$$

Equation (14) describing perturbed distribution function has two distinct parts, one is well known perturbed distribution function in plasma physics and the other arising due to interaction of an external perpendicular a.c. field. Equation (14) reduces to the expression of Landau and Cuperman (1971), Davidson (1983) and Sazhin (1993), when an external a.c. field is set to zero.

The conductivity tensor $\parallel \sigma \parallel$ is written as

$$\begin{aligned} \parallel\sigma\parallel = -i\sum\frac{e_s^2}{m_s\omega}\sum_{m,n,p,q=-\infty}^{\infty}\int d^3\mathbf{v} \\ \times\frac{J_q(\lambda_3)}{\omega-\mathbf{k}_\parallel\mathbf{v}_\parallel-(n+q)\omega_{c_s}+p\nu}\parallel S_{ij}\parallel, \end{aligned} \tag{15}$$

where

$$S_{ij}=\begin{vmatrix} \mathbf{v}_\perp J_n^2 J_P\frac{n}{\lambda_1}\left[\frac{n}{\lambda_1}U^*+\frac{p}{\lambda_2}D\right] & i\mathbf{v}_\perp\frac{n}{\lambda_1}J_n[J_n'J_pU^*+J_nJ_p'D] & \mathbf{v}_\perp J_n^2\frac{n}{\lambda_1}J_p(W_1^*+W_2^*) \\ -i\mathbf{v}_\perp\frac{n}{\lambda_1}J_n[J_n'J_PU^*+J_nJ_p'D] & \mathbf{v}_\perp J_n'[J_n'J_pU^*+J_nJ_p'D] & -i\mathbf{v}_\perp J_nJ_n'J_p(W_1^*+W_2^*) \\ \mathbf{v}_\perp J_n^2J_p\frac{n}{\lambda_1}(W_1^*+W_2^*) & iJ_n\mathbf{v}_\parallel[J_n'J_pU^*+J_nJ_p'D] & \mathbf{v}_\parallel J_n^2(\lambda_1)J_p(\lambda_2)(W_1^*+W_2^*) \end{vmatrix} \tag{16}$$

with

$$\lambda_1=\frac{\mathbf{k}_\perp\mathbf{v}_\perp}{\omega_{c_s}},\quad \lambda_2=\frac{\mathbf{k}_\perp\Gamma_x}{\omega_{c_s}^2-\nu^2},\quad \lambda_3=\frac{\mathbf{k}_\perp\nu\Gamma_x}{\omega_{c_s}(\omega_{c_s}^2-\nu^2)}$$

$$\xi=\frac{\omega-n\omega_{c_s}+\nu}{\mathbf{k}_\parallel\theta_{\parallel_s}},$$

$$C = (\omega - \mathbf{k}_\parallel \mathbf{v}_\parallel)\mathbf{v}_\perp \frac{1}{|\mathbf{v}_\perp|}\frac{\partial f_{0s}}{\partial \mathbf{v}_\perp} + \mathbf{k}_\parallel \mathbf{v}_\perp \frac{\partial f_{0s}}{\partial \mathbf{v}_\parallel}$$

$$D = (\omega - \mathbf{k}_\parallel \mathbf{v}_\parallel)\frac{\Gamma_x}{(\omega_{c_s}^2 - \nu^2)}\frac{1}{\mathbf{v}_\perp}\frac{\partial f_{0s}}{\partial \mathbf{v}_\perp} + \mathbf{k}_\parallel \frac{\Gamma_x}{(\omega_{c_s}^2 - \nu^2)}\frac{\partial f_{0s}}{\partial \mathbf{v}_\parallel}$$

$$F = \mathbf{k}_\perp \mathbf{v}_\parallel \mathbf{v}_\perp \frac{1}{|\mathbf{v}_\perp|}\frac{\partial f_{0s}}{\partial \mathbf{v}_\perp} - \mathbf{k}\perp \mathbf{v}_\perp \frac{\partial f_{0s}}{\partial \mathbf{v}_\parallel}$$

$$G = \mathbf{k}_\parallel \mathbf{v}_\parallel \frac{\nu\Gamma_x}{(\omega_{c_s}^2 - \nu^2)}\frac{1}{\mathbf{v}_\perp}\frac{\partial f_{0s}}{\partial \mathbf{v}_\perp} - \frac{\mathbf{k}_\perp \nu\Gamma_x}{(\omega_{c_s}^2 - \nu^2)}\frac{\partial f_{0s}}{\partial \mathbf{v}_\parallel}$$

$$\Gamma_x = \frac{e_s \mathbf{E}_{0x}}{m_s}, \quad J_n' = \frac{\mathrm{d}J_n(\lambda_1)}{\mathrm{d}\lambda_1}, \quad J_p' = \frac{\mathrm{d}J_p(\lambda_2)}{\mathrm{d}\lambda_2}$$

$$C_1 = \frac{1}{\mathbf{v}_\perp}\frac{\partial f_{0s}}{\partial \mathbf{v}_\perp}(\omega - \mathbf{k}_\parallel \mathbf{v}_\parallel) + \mathbf{k}_\parallel \frac{\partial f_{0s}}{\partial \mathbf{v}_\parallel}$$

$$U^* = C_1 \cdot \mathbf{v}_\perp$$

$$D = C_1 \left[\frac{\Gamma_x}{(\omega_{c_s}^2 - \nu^2)} - \frac{\nu\Gamma_x}{(\omega_{c_s}^2 - \nu^2)}\right]$$

$$W_1^* = n\omega_{cs}\frac{\mathbf{v}_\parallel}{\mathbf{v}_\perp}\frac{\partial f_{0s}}{\partial \mathbf{v}_\perp} + \left(1 - \frac{n\omega_{c_s}}{\omega}\right)\frac{\partial f_{0s}}{\partial \mathbf{v}_\parallel}$$

$$W_2^* = \frac{\mathbf{k}_\perp \nu\Gamma_x}{(\omega_{c_s}^2 - \nu^2)}\left(\frac{p}{\lambda_2} - \frac{n}{\lambda_1}\right)\left[n\omega_{c_s}\frac{\mathbf{v}_\parallel}{\mathbf{v}_\perp}\frac{\partial f_{0s}}{\partial \mathbf{v}_\perp} + \left(1 - \frac{n\omega_{c_s}}{\omega}\right)\frac{\partial f_{0s}}{\partial \mathbf{v}_\parallel}\right].$$

The generalized dielectric tensor for parallel propagating whistler waves in the presence of perpendicular a.c. electric field have been obtained by substituting the limit of $\mathbf{k}_\perp \to 0$, $\mathbf{k} = k_\parallel \hat{e}_z$, into the dielectric tensor given by Summers et al. (1994).

For whistler mode instability the elements of dielectric tensor obtained from (16) get simplified and dispersion relation reduces to

$$\begin{vmatrix} -N_\parallel^2 + \epsilon_{11} & \epsilon_{12} & 0 \\ -\epsilon_{12} & -N_\parallel^2 + \epsilon_{22} & 0 \\ 0 & 0 & \epsilon_{33} \end{vmatrix} = 0. \tag{17}$$

Above expression is rewritten in a more convenient form for right and left handed polarized whistler waves as

$$N_\parallel^4 - 2\epsilon_{11}N_\parallel^2 + \epsilon_{11}^2 + \epsilon_{12}^2 = 0 \tag{18}$$

and for electrostatic waves

$$\epsilon_{33} = 0. \tag{19}$$

The use of particle velocity distribution function (5) reduces the dielectric tensor in the presence of perpendicular a.c. field as

$$\epsilon_{11} = 1 + \sum_s \frac{\omega_{p_s}^2}{\omega^2} \sum_{n=-\infty}^{+\infty} n^2 \times \left\{ A_{T_s}^{\kappa} S_1 + \left(A_{T_s}^{\kappa} \xi_{ns} + \frac{\omega}{\mathbf{k}_{\|} \theta_{\|_s}} \right) S_2 \right\} \tag{20}$$

$$\epsilon_{11} = \epsilon_{22} \tag{21}$$

$$\epsilon_{12} = \sum_s \frac{\omega_{p_s}^2}{\omega^2} \sum_{n=-\infty}^{+\infty} in \times \left\{ A_{T_s}^{\kappa} S_3 + \left(A_{T_s}^{\kappa} \xi_{ns} + \frac{\omega}{\mathbf{k}_{\|} \theta_{\|_s}} \right) S_4 \right\}, \tag{22}$$

where

$$S_1 = \frac{\left(\kappa - \frac{3}{2}\right)\left(\kappa - \frac{5}{2}\right)}{(\kappa - 2)^2} \int_0^{\infty} \lambda_1 J_n^2(\lambda_1)\, \mathrm{d}\lambda_1$$

$$S_2 = \left(\frac{\kappa - 1}{\kappa - 2} \right)^{3/2} \left(\frac{\kappa - \frac{5}{2}}{\kappa - 2} \right)$$

$$\times \left[\left\{ \int_0^{\infty} \lambda_1 J_n^2(\lambda_1) Z_{\kappa-1}^*((\kappa - 1)/(\kappa - 2))^{1/2} \xi_{ns} \right\} \mathrm{d}\lambda_1 \right.$$

$$\left. + \frac{\nu \Gamma_x}{(\omega_{c_s}^2 - \nu^2)} \{ J_p'(\lambda_2) Z_{\kappa-1}^*((\kappa - 1)/(\kappa - 2))^{1/2} \xi_{ns} \}\, \mathrm{d}\lambda_2 \right]$$

$$S_3 = \frac{\left(\kappa - \frac{3}{2}\right)\left(\kappa - \frac{5}{2}\right)}{(\kappa - 2)^2} \int_0^{\infty} \lambda_1^2 J_n(\lambda_1) J_n'(\lambda_1)\, \mathrm{d}\lambda_1$$

$$S_4 = \left(\frac{\kappa - 1}{\kappa - 2} \right)^{3/2} \left(\frac{\kappa - \frac{5}{2}}{\kappa - 2} \right)$$

$$\times \left[\left\{ \int_0^{\infty} \lambda_1^2 J_n(\lambda_1) J_n'(\lambda_1) Z_{\kappa-1}^*((\kappa - 1)/(\kappa - 2))^{1/2} \xi_{ns} \right\} \mathrm{d}\lambda_1 \right.$$

$$\left. + \frac{\nu \Gamma_x}{(\omega_{c_s}^2 - \nu^2)} \{ J_p(\lambda_2) Z_{\kappa-1}^*((\kappa - 1)/(\kappa - 2))^{1/2} \xi_{ns} \}\, \mathrm{d}\lambda_2 \right],$$

where $J_n(\lambda_1)$ and $J_p(\lambda_2)$ are the Bessel function of first kind order n (for the cyclotron harmonic $n = 0, \pm 1, \pm 2 \ldots$), $J_n'(\lambda_1)$ and $J_p'(\lambda_2)$ are the derivatives with respect to λ_1 and λ_2.

The value of integral $S_1, S_2, \ldots, S_4$ contains Bessel function, spectral index κ, modified plasma dispersion function $Z_\kappa^*(\xi)$ and the contribution of perpendicular a.c. electric field. In the presence of perpendicular a.c. electric field the modified plasma dispersion function is also correspondingly modified. The integrals S_1, S_2, $\ldots S_4$ reduce to power series form in the limit of $\lambda \to 0$ and $\mathbf{k}_\perp \to 0$, as given by Summers et al. (1994) in the presence of perpendicular a.c. electric field gets modified as

$$S_1 = S_3 = \frac{1}{2^{|n|}} \frac{\kappa^{|n|-1}\Gamma\left(\kappa - |n| + \frac{1}{2}\right)}{\Gamma(|n|+1)\Gamma\left(\kappa - \frac{1}{2}\right)} + \cdots \text{if } \kappa > |n| - \frac{1}{2}, \tag{23}$$

$$S_2 = S_4 = \left(1 + \frac{\nu\Gamma_x}{(n\omega_{c_s}^2 - \nu^2)}\right) \frac{1}{2^{|n|}} \frac{\kappa^{|n|}\Gamma\left(\kappa - |n| - \frac{1}{2}\right)}{\Gamma(|n|+1)\Gamma\left(\kappa - \frac{1}{2}\right)} \left(\frac{\kappa - |n|}{\kappa}\right)^{3/2}$$

$$Z_{\kappa-|n|}^* \left[\left(\frac{\kappa - |n|}{\kappa}\right)^{1/2} \xi_{ns}\right] + \cdots \text{if } \kappa \geq |n| + 1. \tag{24}$$

The function $Z_{\kappa-1}^*$ occurring in (24) is the modified plasma dispersion function with changed ξ given by Summers and Thorne (1991)

$$Z_\kappa^*(\xi) = \frac{1}{\sqrt{\pi}} \frac{\Gamma(\kappa+1)}{\kappa^{3/2}\Gamma\left(\kappa - \frac{1}{2}\right)} \times \int_{-\infty}^{+\infty} \frac{\mathrm{d}t}{(t-\xi)\left(1 + \frac{t^2}{\kappa}\right)^{\kappa+1}}, \text{Im}(\xi) > 0, \tag{25}$$

valid for positive integral values of κ, with $\xi = x + iy$. Following Summers and Thorne (1991) for integral values of $\kappa > 3/2$, Z_κ^* expressed in closed form of finite series as:

$$Z_\kappa^*(\xi) = -\frac{\left(\kappa - \frac{1}{2}\right)}{2\kappa^{3/2}} \frac{\kappa!}{(2\kappa)!} \times \sum_{\ell=0}^{\kappa} \frac{(\kappa+\ell)!}{\ell!} i^{\kappa-\ell} \left(\frac{2}{(\xi/\sqrt{\kappa}) + i}\right)^{\kappa+1-\ell}. \tag{26}$$

Power series expansion of modified plasma dispersion function $Z_\kappa^*(\xi)$ for small argument $\xi \to 0$ and large argument $\xi \to \infty$ is given in Summers and Thorne

(1991). In this case the power series expansion of $Z_\kappa^*(\xi)$ (valid for all positive integral κ) for large argument $\xi \to \infty$ is given as:

$$Z_\kappa^*(\xi) = \frac{\kappa!\kappa^{\left(\kappa-\frac{1}{2}\right)}\sqrt{\pi}\,i}{\Gamma\left(\kappa-\frac{1}{2}\right)}\frac{1}{\xi^{2(\kappa+1)}}\left(1-\frac{\kappa(\kappa+1)}{\xi^2}+\cdots\right)-\frac{(2\kappa-1)}{(2\kappa)}\frac{1}{\xi}$$
$$\times\left[1+\left(\frac{\kappa}{2\kappa-1}\right)\frac{1}{\xi^2}+\frac{3\kappa^2}{(2\kappa-1)(2\kappa-3)}\frac{1}{\xi^4}+\cdots\right],\ |\xi|\to\infty. \tag{27}$$

The real and imaginary parts of the series are readily available from this expression. This above expression is substituting in S_2 and S_4 in Equation (24). Substituting the values of integrals S_1, S_2, S_3 and S_4 into Equations (20) and (22), the desired elements of dielectric tensors are obtained. Subsequently these dielectric tensor elements are put into Equation (18) to obtain the resulting dispersion relation for right handed polarized whistler mode wave propagating parallel to magnetic field in the presence of perpendicular a.c. field. In case higher powers of **N** are neglected in Equation (18) the dispersion relation for whistler wave reduces to

$$\frac{c^2\mathbf{k}_\parallel^2}{\omega^2} = 1+\sum_s\frac{\omega_{p_s}^2}{\omega^2}\left(\frac{\omega}{\mathbf{k}_\parallel\theta_{\parallel_s}}\frac{\kappa}{\kappa-\frac{3}{2}}\left(\frac{\kappa-1}{\kappa}\right)^{3/2}\right.$$
$$\times Z_{\kappa-1}^*\left[\sqrt{\frac{\kappa-1}{\kappa}}\left(\frac{\omega-n\omega_{c_s}+\nu}{\mathbf{k}_\parallel\theta_{\parallel_s}}\right)\right]$$
$$+A_{T_s}^\kappa\left\{1+\frac{\kappa-1}{\kappa-\frac{3}{2}}\sqrt{\frac{\kappa-1}{\kappa}}\left(\frac{\omega-n\omega_{c_s}+\nu}{\mathbf{k}_\parallel\theta_{\parallel_s}}\right)\right.$$
$$\times Z_{\kappa-1}^*\left[\sqrt{\frac{\kappa-1}{\kappa}}\left(\frac{\omega-n\omega_{c_s}+\nu}{\mathbf{k}_\parallel\theta_{\parallel_s}}\right)\right]\Bigg\}$$
$$+\frac{\nu\Gamma_x}{2(n\omega_{c_s}^2-\nu^2)\theta_{\perp_s}}\left\{\frac{\omega}{\mathbf{k}_\parallel\theta_{\parallel_s}}\frac{\kappa}{\kappa-\frac{3}{2}}\left(\frac{\kappa-1}{\kappa}\right)^{3/2}\right.$$
$$\times Z_{\kappa-1}^*\left[\sqrt{\frac{\kappa-1}{\kappa}}\left(\frac{\omega-n\omega_{c_s}+\nu}{\mathbf{k}_\parallel\theta_{\parallel_s}}\right)\right]$$

$$+ A_{T_s}^{\kappa}\left(1 + \frac{\kappa - 1}{\kappa - \frac{3}{2}}\sqrt{\frac{\kappa - 1}{\kappa}}\left(\frac{\omega - n\omega_{c_s} + \nu}{\mathbf{k}_{\parallel}\theta_{\parallel_s}}\right)\right.$$

$$\left.\times Z_{\kappa-1}^{*}\left[\sqrt{\frac{\kappa - 1}{\kappa}}\left(\frac{\omega - n\omega_{c_s} + \nu}{\mathbf{k}_{\parallel}\theta_{\parallel_s}}\right)\right]\right)\Bigg\}\Bigg). \tag{28}$$

For cold plasma injection, the well known cold plasma dispersion relation of whistler wave is added to this dispersion relation. The combined dispersion relation for the warm background plasma characterized by

$$\omega_{p,w} = \left(\frac{4\pi N_w e_s^2}{m}\right)^{1/2}$$

and an injected cold plasma characterized by

$$\omega_{p,c} = \left(\frac{4\pi N_c e_s^2}{m}\right)^{1/2}$$

is written as

$$\frac{c^2\mathbf{k}_{\parallel}^2}{\omega^2} = 1 + \sum_{s=i,e}\frac{\omega_{p_s}^2}{\omega^2}\left(\frac{\omega}{\mathbf{k}_{\parallel}\theta_{\parallel_s}}\frac{\kappa}{\kappa - \frac{3}{2}}\left(\frac{\kappa - 1}{\kappa}\right)^{3/2}\right.$$

$$Z_{\kappa-1}^{*}\left[\sqrt{\frac{\kappa - 1}{\kappa}}\left(\frac{\omega - n\omega_{c_s} + \nu}{\mathbf{k}_{\parallel}\theta_{\parallel_s}}\right)\right]$$

$$+ A_{T_s}^{\kappa}\left\{1 + \frac{\kappa - 1}{\kappa - \frac{3}{2}}\sqrt{\frac{\kappa - 1}{\kappa}}\left(\frac{\omega - n\omega_{c_s} + \nu}{\mathbf{k}_{\parallel}\theta_{\parallel_s}}\right)\right.$$

$$\left.\times Z_{\kappa-1}^{*}\left[\sqrt{\frac{\kappa - 1}{\kappa}}\left(\frac{\omega - n\omega_{c_s} + \nu}{\mathbf{k}_{\parallel}\theta_{\parallel_s}}\right)\right]\right\}$$

$$+ \frac{\nu\Gamma_x}{2(n\omega_{c_s}^2 - \nu^2)\theta_{\perp_s}}\left\{\frac{\omega}{\mathbf{k}_{\parallel}\theta_{\parallel_s}}\frac{\kappa}{\kappa - \frac{3}{2}}\left(\frac{\kappa - 1}{\kappa}\right)^{3/2}\right.$$

$$\left.\times Z_{\kappa-1}^{*}\left[\sqrt{\frac{\kappa - 1}{\kappa}}\left(\frac{\omega - n\omega_{c_s} + \nu}{\mathbf{k}_{\parallel}\theta_{\parallel_s}}\right)\right]\right.$$

$$+ A_{T_s}^{\kappa}\left(1+\frac{\kappa-1}{\kappa-\frac{3}{2}}\sqrt{\frac{\kappa-1}{\kappa}}\left(\frac{\omega-n\omega_{c_s}+\nu}{\mathbf{k}_{\parallel}\theta_{\parallel_s}}\right)\right.$$

$$\left.\times Z_{\kappa-1}^{*}\left[\sqrt{\frac{\kappa-1}{\kappa}}\left(\frac{\omega-n\omega_{c_s}+\nu}{\mathbf{k}_{\parallel}\theta_{\parallel_s}}\right)\right]\right)\Bigg\}\Bigg)$$

$$-\frac{\omega_{p_{s,c}}^2}{\omega}\frac{1}{(\omega-n\omega_{c_s})} \tag{29}$$

or

$$\frac{c^2\mathbf{k}_{\parallel}^2}{\omega_{p_s,w}^2}=\left(\frac{\omega}{\mathbf{k}_{\parallel}\theta_{\parallel_s}}\frac{\kappa}{\kappa-\frac{3}{2}}\left(\frac{\kappa-1}{\kappa}\right)^{3/2}\right.$$

$$\times Z_{\kappa-1}^{*}\left[\sqrt{\frac{\kappa-1}{\kappa}}\left(\frac{\omega-n\omega_{c_s}+\nu}{\mathbf{k}_{\parallel}\theta_{\parallel_s}}\right)\right]$$

$$+ A_{T_s}^{\kappa}\left\{1+\frac{\kappa-1}{\kappa-\frac{3}{2}}\sqrt{\frac{\kappa-1}{\kappa}}\left(\frac{\omega-n\omega_{c_s}+\nu}{\mathbf{k}_{\parallel}\theta_{\parallel_s}}\right)\right.$$

$$\left.\times Z_{\kappa-1}^{*}\left[\sqrt{\frac{\kappa-1}{\kappa}}\left(\frac{\omega-n\omega_{c_s}+\nu}{\mathbf{k}_{\parallel}\theta_{\parallel_s}}\right)\right]\right\}$$

$$+\frac{\nu\Gamma_x}{2(n\omega_{c_s}^2-\nu^2)\theta_{\perp_s}}\left\{\frac{\omega}{\mathbf{k}_{\parallel}\theta_{\parallel_s}}\frac{\kappa}{\kappa-\frac{3}{2}}\left(\frac{\kappa-1}{\kappa}\right)^{3/2}\right.$$

$$\times Z_{\kappa-1}^{*}\left[\sqrt{\frac{\kappa-1}{\kappa}}\left(\frac{\omega-n\omega_{c_s}+\nu}{\mathbf{k}_{\parallel}\theta_{\parallel_s}}\right)\right]$$

$$+ A_{T_s}^{\kappa}\left(1+\frac{\kappa-1}{\kappa-\frac{3}{2}}\sqrt{\frac{\kappa-1}{\kappa}}\left(\frac{\omega-n\omega_{c_s}+\nu}{\mathbf{k}_{\parallel}\theta_{\parallel_s}}\right)\right.$$

$$\left.\left.\times Z_{\kappa-1}^{*}\left[\sqrt{\frac{\kappa-1}{\kappa}}\left(\frac{\omega-n\omega_{c_s}+\nu}{\mathbf{k}_{\parallel}\theta_{\parallel_s}}\right)\right]\right)\right\}\Bigg)$$

$$-\delta\frac{\omega}{(\omega-n\omega_{c_s})}, \tag{30}$$

where $\delta = \frac{N_c}{N_w}$ is the ratio of cold and warm plasma density.

Now when the a.c. field contribution and the ratio of cold and warm plasma density are set to zero, it reduces to the form given earlier (Abraham-Shrauner and Feldman, 1977; Summers and Thorne, 1991; Summers et al., 1994). In this case the most important differences in the dispersion relation lies in the fact that the argument of Bessel function is determined by the amplitude and frequency of the external a.c. signal. The modified plasma dispersion function is also modified accordingly by the frequency of the a.c. signal (Misra and Haile, 1993; Misra and Pandey, 1995).

For analytical comparison with Maxwellian plasma dispersion relation, the κ distribution function (5) and modified plasma dispersion function (25) are reduced to pure bi-Maxwellian distribution function and plasma dispersion function (Fried and Conte, 1961) under the limit $\kappa \to \infty$. Subsequently using Equations (20) to (24) in this limit and thereby evaluating dielectric tensor and dispersion relation given in (18) to (22) the dispersion relation (30) immediately gets reduced to the well known form (Misra and Singh, 1980; Misra and Haile, 1993; Misra and Pandey, 1995) as

$$\frac{c^2\mathbf{k}_\parallel^2}{\omega_{p_{s,w}}^2} = \left[\frac{\omega}{\mathbf{k}_\parallel \alpha_{\parallel_s}} Z(\xi) + A_{T_s}^M\{1 + \xi Z(\xi)\} + \frac{\nu\Gamma_x}{2(n\omega_{c_s}^2 - \nu^2)\alpha_{\perp_s}} \times \left\{\frac{\omega}{\mathbf{k}_\parallel \alpha_{\parallel_s}} Z(\xi) + A_{T_s}^M\{1 + \xi Z(\xi)\}\right\}\right] - \delta\frac{\omega}{(\omega - n\omega_{c_s})} \tag{31}$$

with

$$\xi = \frac{\omega - n\omega_{c_s} + \nu}{\mathbf{k}_\parallel \alpha_{\parallel_s}}$$

and

$$Z(\xi) = \frac{1}{\sqrt{\pi}} \int_{-\infty}^{+\infty} \frac{e^{-t^2}}{t - \xi}\, \mathrm{d}t, \mathrm{Im}(\xi) > 0. \tag{32}$$

This expression further reduces to the results obtained earlier when contribution of external electric field is put to zero (Landau and Cuperman, 1974; Misra and Singh, 1980).

3. Results and Discussion

A numerical procedure using computer technique without any other numerical approximations for numerical evaluation of normalized temporal growth rate for

Whistler waves in the presence of cold plasma injection to background hot generalized bi-Lorentzian (κ) distribution function in the presence of perpendicular a.c. electric field, for magnetospheric conditions, have been carried out from Equation (30) neglecting the contribution of higher harmonics. In order to investigate the effect of various values of a.c. magnitude $\mathbf{E}_0$, a.c. frequency ν, the specific values of spectral index κ and the cold to warm plasma density ratio $\delta = N_c/N_w$ etc. on the dispersion relation at a representative magnetospheric height of $L = 6.6$ with $\mathbf{B}_0 = 10^{-7}$ Tesla is taken. The small change in magnetic field and density pertaining to magnetospheric plasma will yield similar results. The following other plasma parameters are taken as: $T_\parallel = 5$ KeV, temperature anisotropy

$$A_T^\kappa = \left(\frac{T_\perp}{T_\parallel} - 1\right) = 0.25 - 2.00,$$

the magnitude of a.c. field $\mathbf{E}_0 = 10$, 20 and 30 mV/m, the frequency of electric field $\nu = 2$, 4, 6 and 8 KHz, $N_0 = 1 \times 10^6$ m^{-3}, the ratio of cold to warm plasma density $\delta = N_c/N_w = 15$, 30, 45 and 60 and for different positive integral values of spectral index $\kappa = 2, 4, \ldots, \infty$, etc. The calculation of normalized temporal growth rate for the real values of wave vector $\mathbf{k}$ and complex wave frequency ω is solved numerically by iteration on ω. The function $Z^*_{\kappa-1}(\xi)$ occurring in dispersion relation (30) may be calculated numerically by the power series expansion of $Z^*_\kappa(\xi)$ under the restricted conditions of $\kappa \geq 3/2$ and $\lambda \to 0$ and $n = 1$ (the first harmonics of the cyclotron and the external a.c. field frequencies) and the results are shown in a series of curves (Figures 1–4).

Figures 1a, b shows the dependence of normalized temporal growth rate $\bar{\gamma} = (\omega_i/\omega_c)$ of whistler waves on the normalized wave vector $\bar{\mathbf{K}} = (\mathbf{k}_\parallel \theta_\parallel/\omega_c)$ for various ratios of cold to warm plasma density $\delta = (N_c/N_w)$ at a fixed temperature anisotropy $A_T = 0.75$, electric field magnitude $\mathbf{E}_0 = 20$ mV/m and frequency of electric field $\nu = 2$ KHz for bi-Lorentzian (κ) plasma with spectral index $\kappa = 2$ as well as for bi-Maxwellian plasma ($\kappa = \infty$) respectively. In both cases i.e., the bi-Lorentzian (κ) plasma as well as bi-Maxwellian plasma, the injection of cold plasma to background hot plasma, increases the growth rate by an order of magnitude even when cold plasma density is 15 times larger than warm plasma density. The maximum value of growth rate is slightly larger in case of bi-Lorentzian (κ) plasma than for those of bi-Maxwellian plasma. The increase in the ratio of cold to warm plasma density, over certain limit, the growth rate decreases and emission frequencies of whistler mode instability corresponding to maxima of growth rate shifts towards lower values of $\bar{\mathbf{K}}$. Thus a physical situation like this may explain emission of various whistler frequencies by cold plasma injection. In the case of bi-Maxwellian plasma, the growth rate is little smaller than for those of bi-Lorentzian (κ) plasma and the emission frequency also changes from higher values to lower values of $\bar{\mathbf{K}}$ space. However, in bi-Lorentzian (κ) plasma in power series expansion of integral, $Z^*_\kappa(\xi)$ and spectral index κ increases the perpendicular thermal velocity

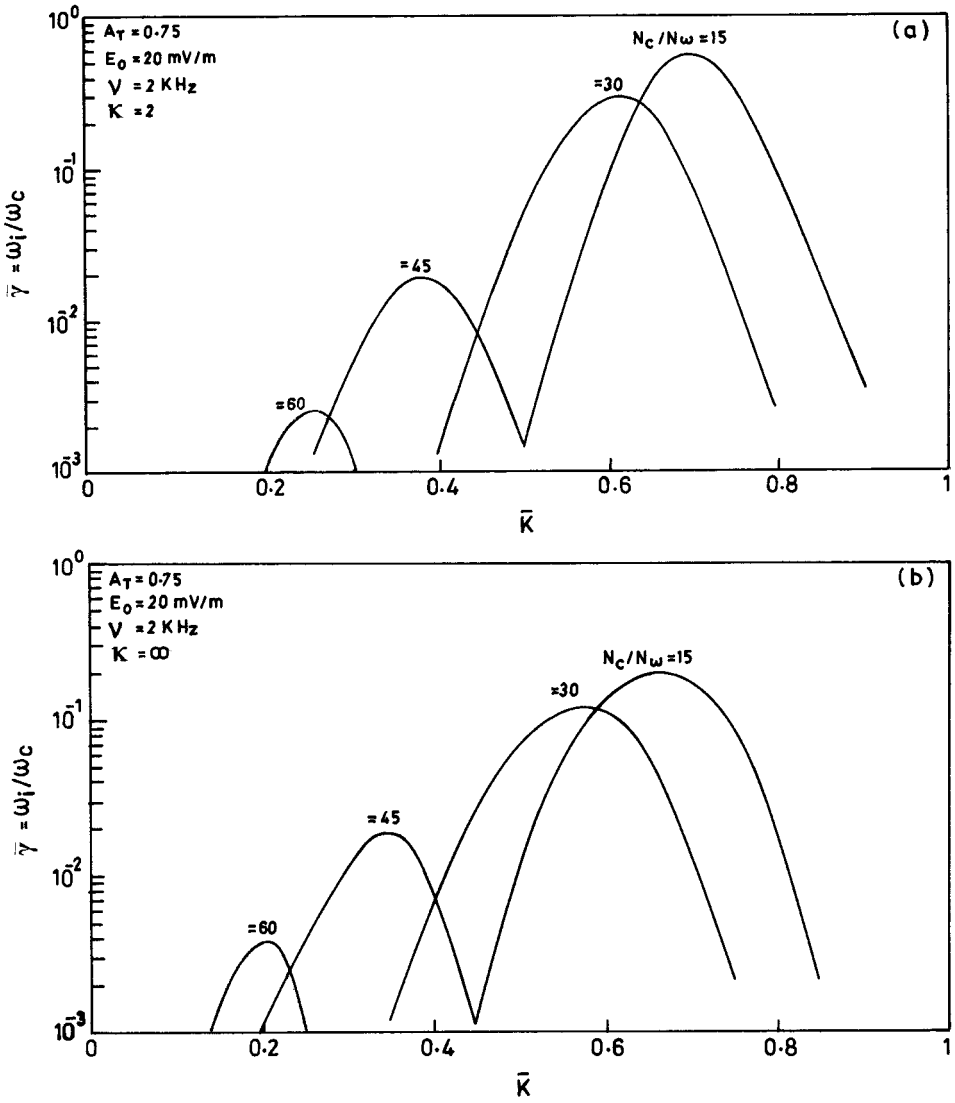

Figure 1. Dependence of the normalized temporal growth rate $\bar{\gamma}$ on the normalized wave number $\bar{\mathbf{K}} = (\mathbf{k}_\parallel \theta_\parallel/\omega_c)$ of Whistler waves for various ratios of cold and warm plasma density (N_c/N_w) in the case of (a) bi-Lorentzian (κ) plasma for $\kappa = 2$, and (b) bi-Maxwellian plasma when $\kappa = \infty$.

$\theta_\perp$ and perpendicular particle velocity $v_\perp$ gives an increase of temperature anisotropy. Thus giving an additional increase in perpendicular thermal velocity than the already existing temperature anisotropy, which is a source of free energy. Thus for bi-Lorentzian (κ) plasma there is an increase in source of energy and increased number of resonant particles in the high energy tail giving rise to enhancement in growth rate.

Figures 2a, b give the variation of normalized growth rate $\bar{\gamma}$ with normalized wave vector $\bar{\mathbf{K}}$ for various values of a.c. frequencies for bi-Lorentzian (κ) plasma ($\kappa = 2$) as well as bi-Maxwellian plasma $\kappa = \infty$ for a fixed value of temperature anisotropy $A_T = 0.5$, the magnitude of a.c. field $\mathbf{E}_0 = 20$ mV/m and the ratio of cold to warm plasma density $N_c/N_w = 30$ are given in figure captions. It is observed that the value of maximum growth rate increases significantly corresponding to increases in the a.c. frequencies from 2 KHz to 8 KHz and the growth rate in this case is substantially higher for bi-Lorentzian (κ) plasma than for bi-Maxwellian plasma. The unstable spectrum of whistler emission shift in $\bar{\mathbf{K}}$ space towards the lower value of $\bar{\mathbf{K}}$ (higher frequency) in both cases of bi-Lorentzian (κ) plasma as well as bi-Maxwellian plasma. The shift in K values is more pronounced for bi-Maxwellian plasma than for bi-Lorentzian (κ) plasma. The variation of normalized frequency $x = (\omega_r/\omega_c)$ with normalized wave number $\bar{\mathbf{K}}$ can easily determine the values of generated frequencies where the peak of growth rate cuts the real frequency curve. Thus the generated real frequency in case of bi-Lorentzian (κ) plasma is ranging from 11.26 KHz to 13.37 KHz and for bi-Maxwellian plasma it ranges 10.91 KHz to 12.67 KHz corresponding to a.c. frequency changing from 2 KHz to 8 KHz.

Figures 3a, b show the variation of normalized temporal growth rate $\bar{\gamma}$ with the ratio of cold to warm plasma density N_c/N_w for various values of temperature anisotropy A_T where $\mathbf{E}_0 = 10$ mV/m, $\nu = 2$ KHz for both bi-Lorentzian (κ) plasma ($\kappa = 2$) as well as for bi-Maxwellian plasma ($\kappa = \infty$). In this calculation the values of $\bar{\mathbf{K}}$ corresponding to growth maxima are taken from previous Figures 1a, b corresponding to the ratio of cold to warm plasma density N_c/N_w at this a.c. frequency $\nu = 2$ KHz. In both cases growth rate increases with increases in the temperature anisotropy but the maxima are found to exist at different ratios of cold to warm plasma density N_c/N_w. These observations imply that both the thermal anisotropy A_T and the injected cold plasma are the major source of free energy for seeding the instability. The maximum growth rate expression corresponding to a given value of N_c/N_w has been obtained earlier by Cuperman and Landau (1974). Following their methodology our $\bar{\mathbf{K}}$ maxima agree with their results. The cold electron density controls which frequency band should be excited. The cutoff existing for values of N_c/N_w is in the range of 40-45, the increase in this ratio increases the group velocity, thus limiting the excited frequencies.

Figures 4a, b show the variation of normalized temporal growth rate $\bar{\gamma}$ with the ratio of cold to warm plasma density N_c/N_w for various values of magnitude of a.c. electric field at a fixed temperature anisotropy $A_T = 0.50$, frequency of electric field $\nu = 2$ KHz for both bi-Lorentzian (κ) plasma as well as bi-Maxwellian plasma. In this calculation the value of $\bar{\mathbf{K}}$ at maximum growth rate is taken from previous Figures 3a, b corresponding to the ratio of cold to warm plasma density N_c/N_w at a.c. frequency $\nu = 2$ KHz. In both cases the magnitude of a.c. electric field shows the sharp enhancement to growth rate for the lower ratios of cold to warm plasma density N_c/N_w. Further increase in a.c. magnitude in case of both

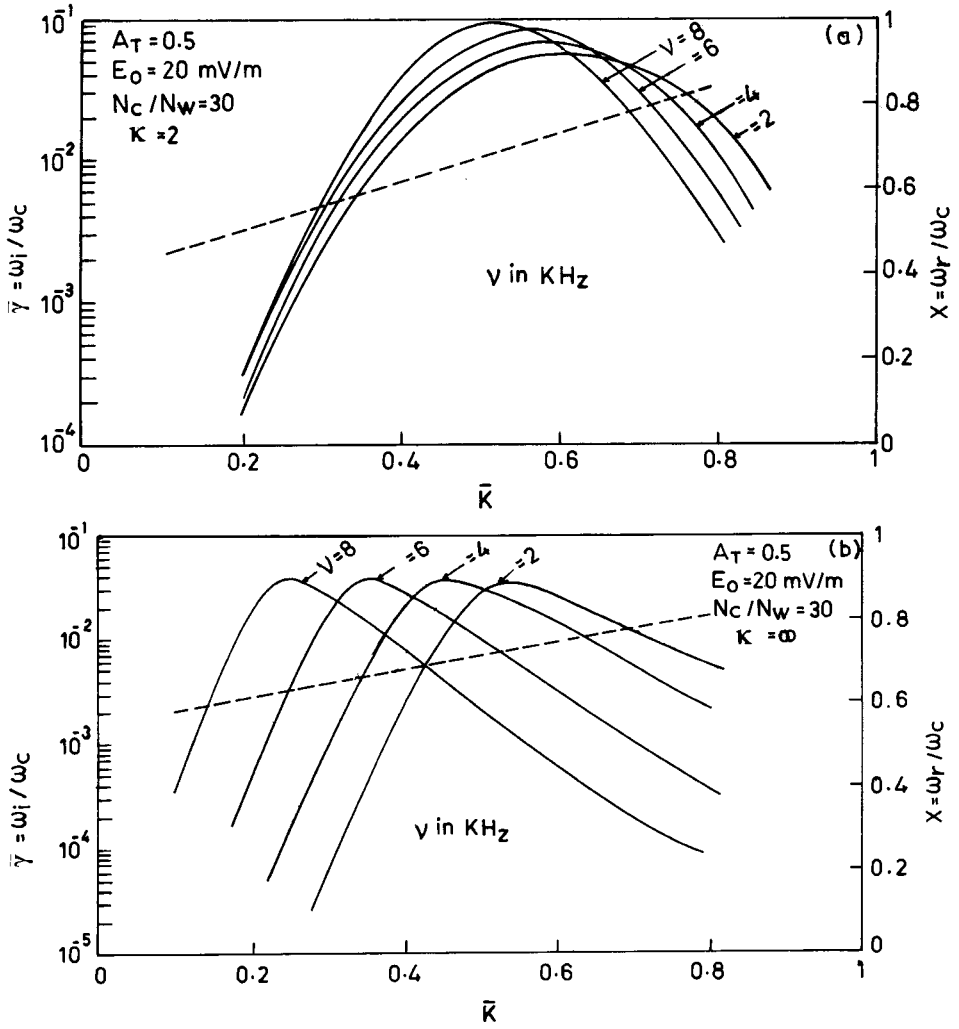

Figure 2. The normalized temporal growth rate $\bar{\gamma}$ (solid lines) and the normalized real frequency x (dotted lines) of whistler waves as functions of normalized wave number $\bar{\mathbf{K}}$ for a fixed injected cold plasma ratio for various values of a.c. field frequency ν in the case of (a) bi-Lorentzian (κ) plasma for $\kappa = 2$ and (b) bi-Maxwellian plasma when $\kappa = \infty$.

plasmas does not show change in growth rate even for higher ratios of cold to warm plasma density.

4. Conclusions

The addition of cold plasma increases the instability range in $\bar{\mathbf{K}}$ space, and this increase in range leads to lower values of $\bar{\mathbf{K}}$ in both cases, i.e., for bi-Lorentzian

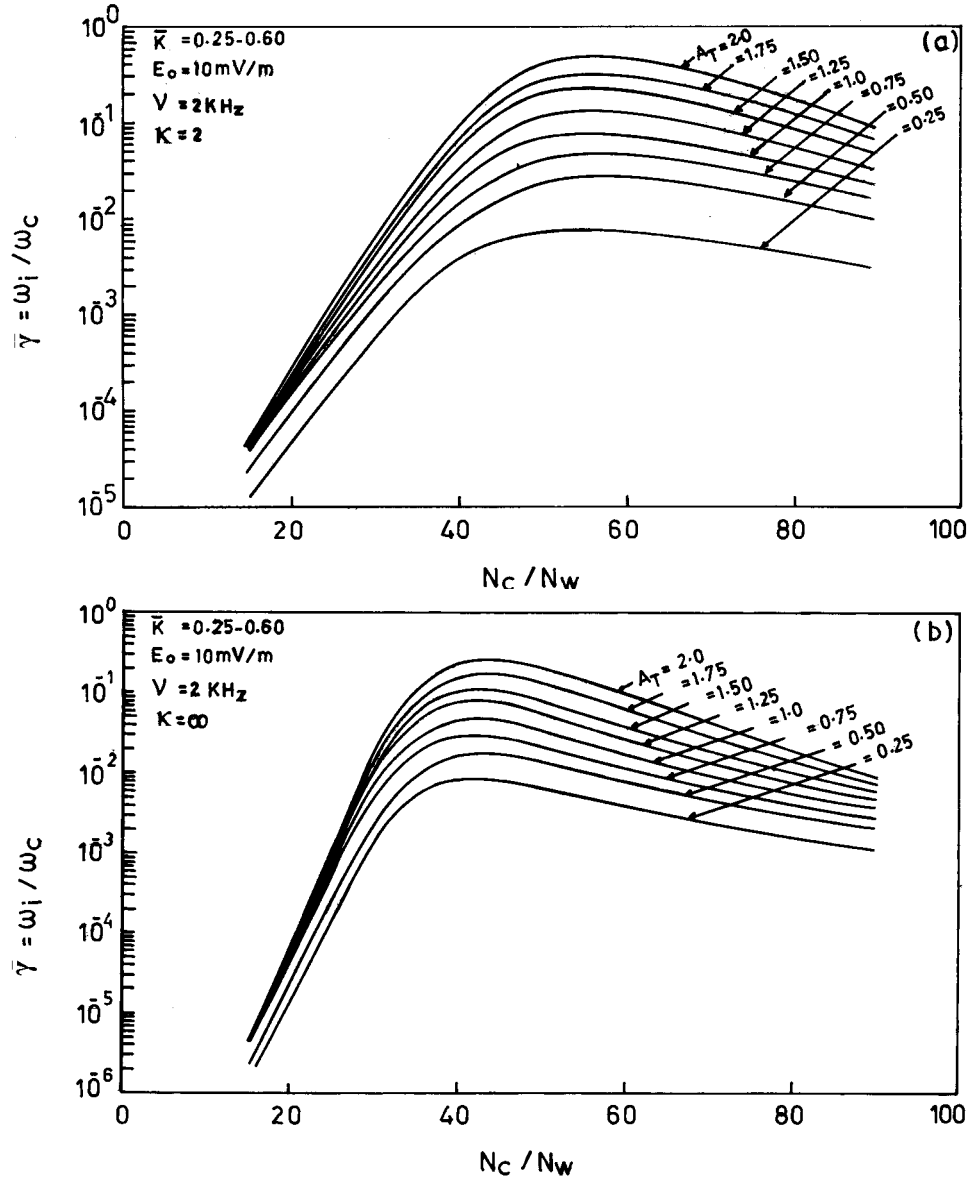

Figure 3. Dependence of the normalized temporal growth rate $\bar{\gamma}$ on the ratios of cold to warm plasma density (N_c/N_w) of whistler wave for various values of temperature anisotropy $A_T = (T_\perp/T_\parallel) - 1$ in the case of (a) bi-Lorentzian (κ) plasma for $\kappa = 2$, and (b) bi-Maxwellian plasma when $\kappa = \infty$.

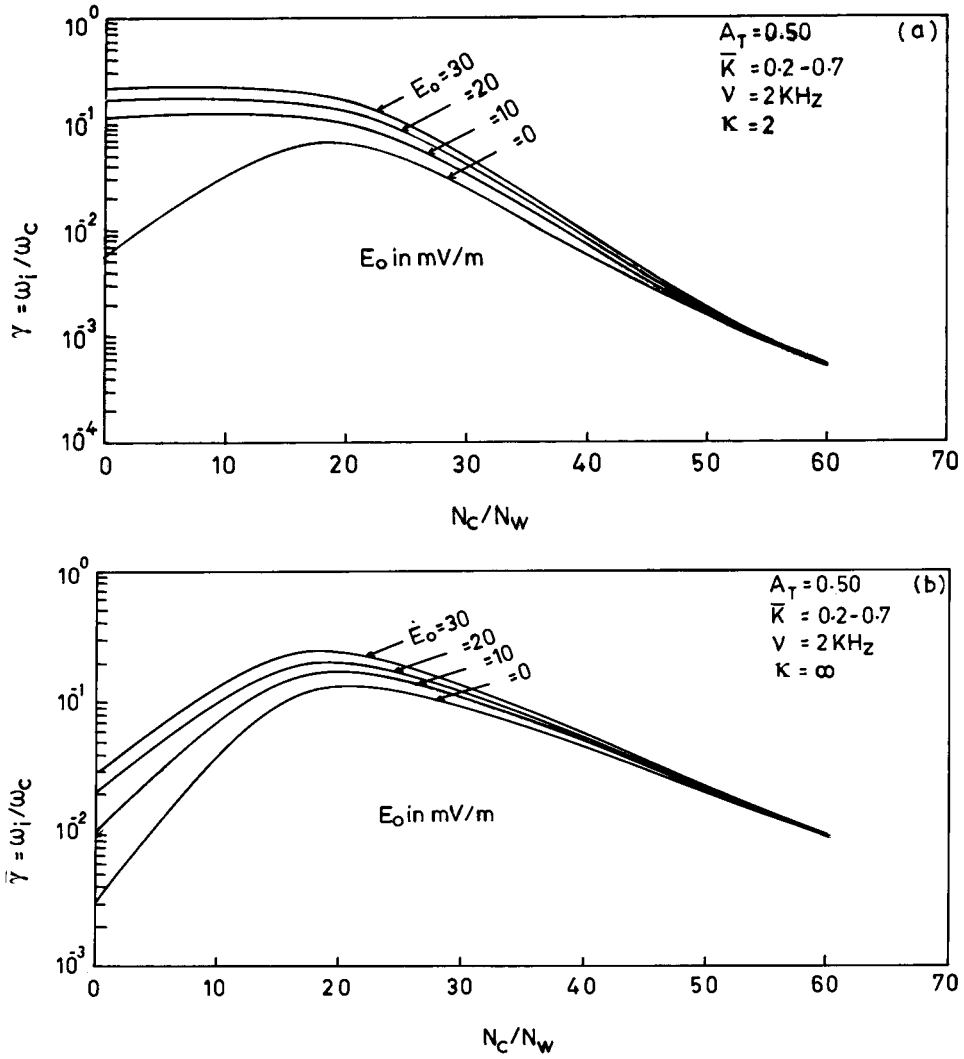

Figure 4. Dependence of the normalized temporal growth rate $\bar{\gamma}$ on the ratios of cold to warm plasma density (N_c/N_w) of whistler wave for various values of a.c. field magnitude E_0 in the case of (a) bi-Lorentzian (κ) plasma for $\kappa = 2$, and (b) bi-Maxwellian plasma when $\kappa = \infty$.

(κ) plasma as well as bi-Maxwellian plasma. Application of perpendicular electric field increases the range of instability in $\bar{\mathbf{K}}$ space, but this increase in range leads to lower values of $\bar{\mathbf{K}}$. The effect of magnitude of perpendicular a.c. electric field is pronounced only for lower values of $\bar{\mathbf{K}}$, N_c/N_w and A_T in both cases. At maximum growth the effect of magnitude of perpendicular a.c. electric field is very small even for higher values of N_c/N_w in both cases. As frequency increases, the range of instability in $\bar{\mathbf{K}}$ space increases, but this increase in $\bar{\mathbf{K}}$ space leads to lower values of $\bar{\mathbf{K}}$ for both cases. The effect of frequency of a.c. field is pronounced only at lower

values of $\bar{\mathbf{K}}$, N_c/N_w and A_T in both cases, i.e., for a bi-Maxwellian plasma as well as bi-Lorentzian (κ) plasma. It is found that in case of bi-Lorentzian (κ) plasma the growth rate is a little higher than for bi-Maxwellian plasma. The bi-Lorentzian (κ) plasma adds some additional energy by increasing the perpendicular thermal velocity because of series expansion of integrals, $Z^*_\kappa(\xi)$ and spectral index κ. The source of free energy for the instability are temperature anisotropy and injected cold plasma. The inclusion of temperature anisotropy and cold plasma injection in bi-Lorentzian (κ) plasma and bi-Maxwellian plasma can explain the observed higher frequencies spectra of whistler waves.

This study may be of potential use in controlled experiments in ionospheric, magnetospheric and laboratory plasma to interpret the dynamic spectra of whistlers observed on the ground and in space while utilizing whistlers for diagnostic purposes during simultaneous injection of cold plasma with ground or *in situ* injection of triggering signals.

Acknowledgement

We gratefully acknowledge the computational help provided by Shri Girish Chandra of I.E.T., Lucknow, India. This work could not have progressed without his help.

References

Abraham-Shrauner, B. and Feldman, W. C.: 1977, 'Electromagnetic Ion Cyclotron Wave Growth Rates and their Variation with Velocity Distribution Function', *J. Plasma Phys.* **17**, 123.

Brice, N. M.: 1970, 'Artificial Enhancement of Energetic Particle Precipitation through Cold Plasma Injection: A Technique of Seeding Substorms?', *J. Geophys. Res.* **75**, 4890.

Brice, N. M. and Lucas, C.: 1971, 'Influence of Magnetospheric Convection and Polar Wind Loss of Electrons from the Outer Radiation Belt', *J. Geophys. Res.* **76**, 900.

Briggs, R. J.: 1964, *Electron-Stream Interaction with Plasmas*, MIT Press, Cambridge, MA.

Cairns, I. H. and Nishikawa, K. I.: 1989, 'Simulations Relevant to the Beam Instability in the Foreshock', *J. Geophys. Res.* **94**, 79–88.

Cornwall, J. M.: 1974, 'Magneto Spheric Dynamics with Artificial Plasma Clouds', *Space Sci. Rev.* **15**, 841.

Christon, S. P., Mitchell, D. G., Williams, D. J., Frank, L. A., Huang, C. Y., and Eastman, T. E.: 1988, 'Energy Spectra of Plasma Sheet Ions and Electrons from ∼50 eV/e ∼ 1 MeV during Plasma Temperature Transitions', *J. Geophys. Res.* **93**, 2562.

Cuperman, S. and Landau, R. W.: 1974, 'On the Enhancement of Whistler Mode Instability in the Magnetospheric by Cold Plasma Injection', *J. Geophys. Res.* **79**, 128.

Cuperman, S. and Sternlieb, A.: 1974, 'Obliquely Propagating Unstable Whistler Waves: A Computer Simulation', *J. Plasma Phys.* **11**, 175.

Davidson, R. C.: 1983, 'Kinetic Waves and Instabilities in a Uniform Plasma', in M. N. Rosenbluth and R. Z. Sagdeev (eds.), *Handbook of Plasma Physics*, Vol. 1, North-Holland, New York, pp. 521–555.

Dum, C. T.: 1990a, 'Simulations Studies of Plasma Waves in the Electron Foreshock: The Generation of Langmuir Waves by a Gentle Bump-on-Tail Electron Instability', *J. Geophys. Res.* **95**, 8095.

Dum, C. T.: 1990b, 'Simulations Studies of Plasma Waves in the Electron Foreshock: The Transition from Reactive to Kinetic Instability', *J. Geophys. Res.* **95**, 8111.

Fried, B. D. and Conte, S. D.: 1961, *The Plasma Dispersion Function*, Academic Press, New York.

Ganguli, G., Palmadesso, P., and Fedder, J.: 1984, 'Temporal Evolution of Whistler Growth in a Cold Plasma Injection Experiment', *J. Geophys. Res.* **89**, 7351.

Gary, S. P. and Madland, C. D.: 1985, 'Electromagnetic Electron Temperature Anisotropies Instabilities', *J. Geophys. Res.* **90**, 7607.

Hasegawa, A., Mima, K., and Duong-Van, M.: 1985, 'Plasma Distribution Function in a Superathermal Radiation Field', *Phys. Rev. Lett.* **54**, 2608.

Helliwell, R. A.: 1965, *Whistlers and Related Ionospheric Phenomena*, Stanford University Press, Stanford, CA.

Kennel, C. F. and Petschek, H. E.: 1966, 'A Limit on Stably Trapped Particles Fluxes', *J. Geophys. Res.* **71**, 1.

Landau, R. W. and Cuperman, S.: 1971, 'Stability of Anisotropic Plasmas to Almost Perpendicular Magneto Sonic Waves', *J. Plasma Phys.* **6**, 495.

Liemohn, H. B.: 1974, 'Simulation of VLF Amplification in the Magnetosphere', *Space Sci. Rev.* **15**, 861.

Lui, A. T. Y. and Krimigis, S. M.: 1981, 'Earthward Transport of Energetic Protons in the Earth's Plasma Sheet', *Geophys. Res. Lett.* **8**, 527.

Mace, R. L.: 1999, 'Enhanced Whistler Instability Produced by Suprathermal Electrons Upstream of the Earth's Bow Shock, (Solar Wind Nine)', in *Ninth International Conference, AIP Conference Proceeding (USA)*, No. 471, pp. 479–482.

Misra, K. D. and Haile, T.: 1993, 'Effect of a.c. Electric Field on the Whistler Mode Instability in the Magnetosphere', *J. Geophys. Res.* **98**, 9297.

Misra, K. D. and Haile, T.: 2001a,'Artificially Triggered Whistler Mode Instability in Realistic Model Magnetosphere', *Ann. Geophys.* (in press).

Misra, K. D. and Haile, T.: 2001b, 'Effect of Time-Dependent Cold Plasma Injection on a.c. Field Triggered Whistler Instability in the Magnetosphere', *Ann. Geophys.* (in press).

Misra, K. D. and Pandey, R. S.: 1995, 'Generation of Whistler Emissions by Injection of Hot Electrons in the Presence of a Perpendicular a.c. Electric Field', *J. Geophys. Res.* **100**, 19405.

Misra, K. D. and Singh, B. D.: 1977, 'Electric Field Induced Instability in the Magnetosphere', *J. Geophys. Res.* **82**, 2267.

Misra, K. D. and Singh, B. D.: 1980, 'On the Modifications of the Whistler Mode Instability in the Magnetosphere in the Presence of Parallel Electric Field by Cold Plasma Injection', *J. Geophys. Res.* **85**, 5138.

Misra, K. D., Singh, B. D., and Mishra, S. P.: 1978, 'Beam-Plasma Instability of a Finite Temperature Electromagnetoplasma', *Plasma Phys.* **20**, 1113.

Misra, K. D., Singh, B. D., and Mishra, S. P.: 1979, 'Effects of Parallel Electric Field on Whistler Mode Instability in the Magnetosphere', *J. Geophys. Res.* **84**, 5923.

Nelson, C. Maynard, Burke, William J., and Wilson, Gordon R.: 2000, 'Solar Wind Control of the Penetration of Electric Field in the Inner Magnetosphere', *Adv. Space Res.* **25**, 1393.

Neubert, T. and Banks, P. T.: 1992, 'Recent Results from Studies of Electron Beam Phenomena in Space Plasmas', *Planet. Space Sci.* **40**, 153.

Nishikawa, K.-I., Buneman, O., and Neubert, T.: 1994, 'New Aspects of Whistler Waves Driven by an Electron Beam Studied by a 3-D Electromagnetic Code', *Geophys. Res. Lett.* **21**, 1019.

Omura, Y. and Matsumoto, H.: 1988a, 'Computer Experiments on Whistler and Plasma Wave Emissions for Space Lab-2 Electron Beam', *Geophys. Res. Lett.* **15**, 319.

Omura, Y. and Matsumoto, H.: 1988b, 'Electromagnetic and Electrostatic Emissions from a Thin Electron Beam in Space Plasma', in B. Lembege and J. W. Eastwood (eds.), *Numerical Simulations of Space Plasmas*, North-Holland, New York, p. 133.

Prasad, R.: 1968, 'Instabilities in Parametric Oscillation of a Plasma', *Phys. Fluids B* **11**, 1768.

Sazhin, S. S.: 1993, *Whistler-Mode Waves in a Hot Plasma*, Cambridge University Press, New York.

Sazhin, S. S. and Sazhina, E. M.: 1988, 'Some Particular Case of Oblique Whistler-Mode Propagation in a Hot Anisotropic Plasma', *J. Plasma Phys.* **40**, 69.

Summers, D. and Thorne, R. M.: 1987, 'Analytical Solutions for the Growth of Oblique Waves in a Plasma with a Field-Aligned Beam', *Phys. Fluids B* **30**, 3761.

Summers, D. and Thorne, R. M.: 1991, 'The Modified Plasma Dispersion Function', *Phys. Fluids B* **8**, 1835.

Summers, D. and Thorne, R. M.: 1992, 'A New Tool for Analyzing Microinstabilities in Space Plasmas Modeled by a Generalized bi-Lorentzian (κ) Distribution', *J. Geophys. Res.* **97**, 16827.

Summers, D., Xue, S., and Thorne, R. M.: 1994, 'Calculation of the Dielectric Tensor for a Generalized Bi-Lorentzian (κ) Distribution Function', *Phys. Plasma* **1**, 2012.

Vasyliunas, V. M.: 1968, 'A Survey of Low-Energy Electrons in the Evening Sector of the Magnetosphere with OGO1 and 0G03', *J. Geophys. Res.* **73**, 2839.